ORIGINAL PAPER

Optical, thermophysical and electrical characterization of PMMA (CdSe QDs) composite films

N. M. Al-Hosiny · S. Abdallah · M. A. A. Moussa · Ali Badawi

Abstract The concentration dependence of optical, thermophysical and electrical behavior, based on poly-methyl methacrylate filled with CdSe quantum dots (PMMA (CdSe)) have been investigated. The PMMA(CdSe) concentration was 0.001, 0.005, 0.01 and 0.05 wt.%. The composites were prepared in the form of films by the solution casting technique. The optical properties of PMMA(CdSe) films have showed that, there is a red shift of the absorption and photoluminescence (PL) after the QDs were added into PMMA. The PL peak intensity of the composite was enhanced by ≈ 2.5 times compared to the CdSe QDs. The thermal conductivity (k) was obtained by measuring the thermal diffusivity (α) and thermal effusivity (e) using the photoacoustic (PA) technique. The composites exhibit $\approx$ 120 % improvement in k at 0.05 wt.% . Furthermore, the dc electrical conductivity measurements of pure and doped PMMA, showed that the obtained values were enhanced about four orders of magnitude for the highest concentration compared with pure PMMA at 500 ^{0}C.

N. M. Al-Hosiny · S. Abdallah · M. A. A. Moussa (✉) ·
A. Badawi
Department of Physics, Faculty of Science,
Taif University, Taif, Kingdom of Saudi Arabia
e-mail: moussa1864@yahoo.co.uk

S. Abdallah
Department of Mathematical and Physical Engineering,
Faculty of Engineering (Shoubra), Benha University,
Banha, Egypt

M. A. A. Moussa
Department of Physics, Faculty of Science, Mansoura University,
Mansoura, Egypt

N. M. Al-Hosiny
Physics Department, College of Science, Al Jouf University,
Al Jouf, Saudi Arabia

Introduction

Semiconductor quantum dots (QDs) have attracted great interest in recent years due to their unique photophysical properties, which are attractive to a diverse range of applications [1–3]. Especially, the composite of QDs and organic polymers exhibits excellent potential due to low cost, large area, mechanically flexible devices [4–8]. The PMMA polymer can be used in a wide range of applications which can be even more extended by the incorporation of CdSe QDs into its matrix (composites). Provided that CdSe QDs well-dispersed various physical properties of PMMA such as optical, thermal and electrical properties may be enhanced. Measurement of thermal parameters such as thermal diffusivity (α), thermal effusivity (e) and thermal conductivity (k) for PMMA(CdSe) composite film are very essential for their applications, particularly in the fabrication of devices. α ($m^2 s^{-1}$) is a significant thermophysical parameter which measures how effectively phonons carry heat through the sample. Whereas the measurement of the heat exchange rate or the thermal impedance for heat exchange of a given material is essentially determined by e ($Ws^{1/2}m^{-2}K^{-1}$). e is a relevant thermophysical parameter for surface heating or cooling processes as well as in quenching processes. These quantities are defined by $\alpha = k/\rho c$ and $e = \sqrt{k\rho c}$, where k is the thermal conductivity, c is the specific heat capacity and ρ is the mass density. Knowing α, and e, the sample thermal conductivity can be obtained from the relation $k = e\sqrt{\alpha}$. Apart from the pure academic interest, knowledge of the thermal conductivity (k) of PMMA(CdSe) composite generally, aids in the selection of candidate for engineering applications such as parts of computers and automobile engines. Photoacoustic technique (PA)

is a photothermal detection technique; that is proved to be a powerful tool to study the optical and thermal properties of such materials without particular sample treatment in a nondestructive manner [9–11]. More interest has been paid to electrical transport property of composites which reveals important information about the transport phenomenon and other physical properties. These studies have shown that the electrical properties of the polymers can be improved using various nanoparticle dopant. Due to the strong interaction between insulating polymers and nanoparticles a significant enhancement of electrical properties could take place in the produced composites [12, 13]. Recently, many authors have paid attention to improve the mechanical, optical, thermal and electrical properties of PMMA using CdS, CdSe, ZnO [14, 15]. In their work, the composite films were fabricated by electrospinning technique.

In this study, different levels of CdSe QDs were added to PMMA to form composite films using casting solution technique. The effect of PMMA on the optical feature of CdSe QDs has been investigated. A compression of the absorption – emission spectra is made between the CdSe QDs and the complex PMMA(CdSe). Furthermore, The CdSe QDs concentration dependence of thermophysical (α, e and k) and electrical behavior of composites have been investigated.

Outline of the thermophysical measurement methods

The main idea of PA technique is based on the fact that only the absorbed light is converted to sound. The sample to be studied is placed inside a gas/microphone cell, in which a portion of thermal energy is produced in the sample by light absorption. Subsequent thermalization within the sample produce a pressure fluctuation in the air within the cell which is detected as an acoustic signal by a sensitive microphone attached to the cell. Therefore, the PA signal contains information about the optical absorption within the sample in addition to the way with which the heat is diffused through the sample. Rosencwaig and Gersho (RG) theory of the PA effect [16] shows that the pressure variations depend on the relationship among three parameters with dimensions of length: the sample thickness ℓ the optical absorption length μ_B and the thermal diffusion length $\mu (\mu = (\alpha/\pi f)^{1/2})$, where f is the chopping frequency. Charpentier et al. [17] demonstrated that the pressure variations at the front surface of an optically opaque material ($\ell > \mu_B$) can be written as the product of two terms, one depends on f and the other independent of f. When $f > f_c$ the variations of the frequency dependent term is independent of α and when $f < f_c$ the variations in PA signal depends on α that can be calculated from [18, 19]

$$\alpha = \ell^2 f_c \qquad (1)$$

Here the characteristic frequency f_c is defined as the frequency at which the sample goes from thermally thick (μ) to

thermally thin ($\mu > \ell$) region. At this frequency, a distinct change in the slope of ln f versus ln PA Signal amplitude) plot occurs and knowing ℓ, we can calculate α.

Thermal effusivity can be measured by using a reference material of known effusivity. The following requirements have to be fulfilled to carry out the measurements: (a) the sample should be thermally thick, (b) the sample should be in thermal contact with a thermally thin but optically very opaque (i.e. $\ell \gg \mu_B$)[16] metal foil, (c) the light modulation frequency should be much lower than the critical frequency for the metal foil (to conserve its thermal thin condition). The same conditions should be fulfilled for the reference sample. The PA amplitudes q_s and q_r from both the sample and the reference respectively, covered with the foil are measured. The expressions for the amplitudes can be derived, based on RG theory as shown in and the ratio of the amplitudes, R, can be expressed by the following relation [9, 20].

$$R = \frac{q_s}{q_r} = \sqrt{\frac{w_r^2 + 1}{w_s^2 + 1}} \qquad (2)$$

Where $w_s = (e_s \mu_m / \ell_m e_m) + 1$, and w_r is defined using the same relation with e_r instead of e_s. The subscript m refers to the metal foil and μ_m is its thermal diffusion length ($\mu_m = (\alpha_m / \pi f)^{1/2}$). The thickness, ℓ_m, the thermal effusivity, e_m and the thermal diffusivity α_m of the metal foil as well as the thermal effusivity, e_r of the reference should be known. The sample thermal effusivity (e_s) can be extracted by fitting the experimental results with that mathematical relation.

Experiment

Spherical CdSe colloidal nanocrystals were prepared by a method similar to that of Talapine et al. [21, 22]. The trioctyl-phosphine selenide (TOPSe) and dimethylcadmium were dissolved in trioctylphosphine (TOP) and rapidly injected into a vigorously stirred mixture of Trioctylphosphine oxide (TOPO) and hexadecyleamine (HAD). CdSe QDs sample was obtained from the reaction mixture and immediately cooled and diluted with toluene to stop particle growth followed by centrifugation.

The polymer films were prepared using solution casting method in which PMMA was dissolved in acetone with the ratio 1: 27 by which clear films were obtained. The different CdSe nanoparticle solutions were prepared by dispersing appropriate amount of CdSe in 10 ml acetone and put in high power ultrasonic bath for 30 min then mixed with filtered polymer solution. The produced mixture solutions were ultrasonically for 30 min and filtered. They were filtered and casted in petri dishes and left in air for 3 days. Several films of PMMA + x wt% CdSe, where x=0, 0.001,

0.005, 0.01 and 0.05 wt.% of thicknesses: 46, 77, 68, 72, 80 μm respectively. The dried films were reasonably homogeneous and clear.
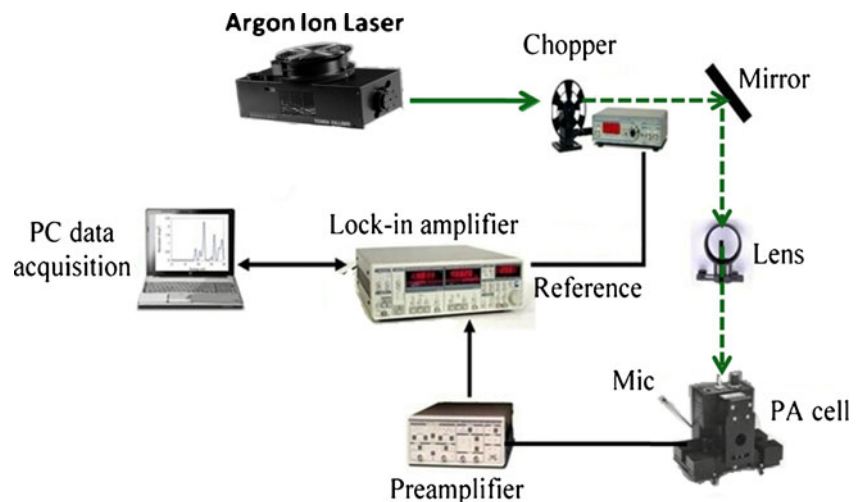
The absorption spectra of CdSe QDs and composite films were determined by a spectrophotometer (JASCO V-670) in the wavelength range from 450 nm to 700 nm. Light emission observed under 472 nm LED lamp.

The PA measurements were carried out by a gas microphone detection technique. The light beam from 200 mW (514 nm) argon ion laser (Melles Griot, Carlsbad, CA 92009) was mechanically modulated by an optical chopper (SR540), and focused onto the sample which was mounted carefully inside a PA cell (MTEC Model 300). The sound wave generated from the sample can be subsequently detected as an acoustic signal by a highly sensitive electrical microphone fixed in the PA cell. The PA signal was then amplified by a low noise preamplifier and further processed using a lock-in amplifier (Stanford Research System, Model SR830 DSP). A personal computer was interfaced to the system for automatic data acquisition and analysis. Figure 1 shows the schematic diagram of the PA experimental set-up for thermal properties measurements. All the measurements were carried out at room temperature.

For thermal effusivity measurements, samples exhibited good adhesion (using silicon grease) to the metal surface ensuring good thermal contact and avoiding the appearance of extra thermal resistance. The used metallic surface was thin aluminum foil ($e_m = 2400 Ws^{1/2}/m^2K$, $\alpha_m = 0.98 \times 10^{-4} m^2/s$ of thickness $\ell_m = 30 \mu m$ and the reference sample was Si wafer of known effusivity (15,670 $Ws^{1/2}/m^2K$) [9, 20, 23].

Dc electrical resistivity was measured in an Oxford Optistat cryostat in the temperature range 300–500 K. An electrometer type Keithly 6517B and an Oxford temperature controller IT053 were connected to a PC computer via GPIB interface TNT5004 card and the data was recorded by a pc. The samples were heated using a constant rate of 1 $^0C/min$.

Results and discussion

Optical measurements

The average particle size distributions of CdSe QDs sample was estimated using transition electron microscopy (TEM), which was about 5.2 nm, as shown in Fig. 2(a). Figure 2(b) shows the UV–vis spectrum of CdSe QDs sample. As can be seen, the absorption edge was 580 nm with a corresponding band gap of 2.12 eV. Such huge blue shift with respect to bulk CdSe (1.74 eV [24]) are considered due to excellent quantum confinement effect.

The particle sizes could be also estimated according to EMA model that gives the energy bands for excitons as a function of nanocrystal radius "R", as [25, 26]
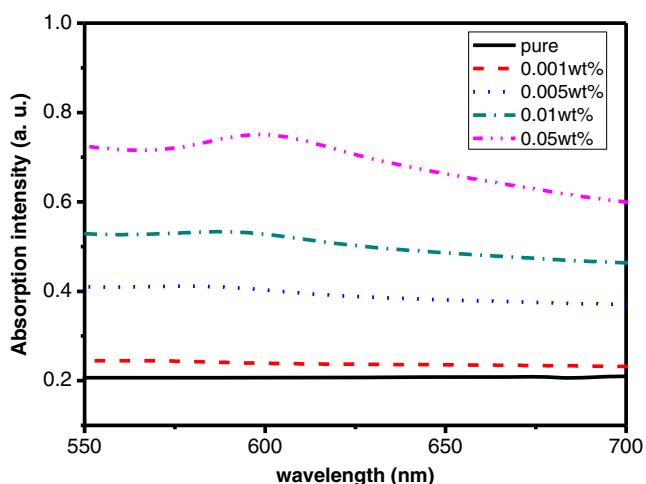
$$E_{g(Nano)} = E_{g(bulk)} + \frac{h^2}{8R^2}\left[\frac{1}{m_e} + \frac{1}{m_h}\right] - \frac{1.8e^2}{4\pi\varepsilon\varepsilon_0 R} \quad (3)$$

where m_e (= 0.13 m_0 [24]) and m_h (= 0.45 m_0 [24]) are the effective masses of electron and hole respectively, m_0 is the free mass of electron, $E_{g (bulk)}$ is the bulk crystal band gap, R is the average radius of the nanocrystal, $E_{g(Nano)}$ is the lowest energy for electronic transition, h is the Planck's constant, ε (= 5.8 [24]) is the relative permittivity, and ε_0 is the vacuum permittivity. The calculated average particle size of CdSe nanocrystal based on the above equation was 5.3 nm which are comparable to those obtained by TEM image.

Figure (3) shows the UV–vis. absorption spectra of the complex PMMA(CdSe) films with 0.001, 0.005, 0.01 and 0.05 wt.% CdSe in PMMA. The effect of varying the amount of QDs in the PMMA and the confinement features were observed at all concentrations although the excitonic peaks in the absorption spectra were not very prominent owing to the small amounts of incorporated QDs. Moreover, the absorption edges of PMMA(CdSe) composite films are red shifted from free CdSe QDs to 606 nm. The red shifts are due to the slight

Fig. 1 The schematic diagram of the PA experimental set-up for thermal measurements
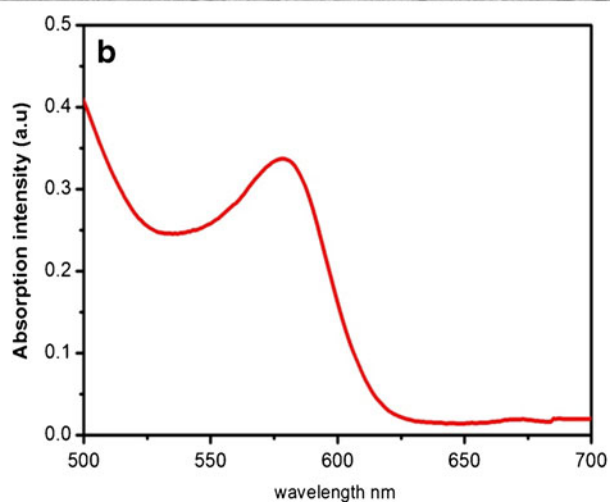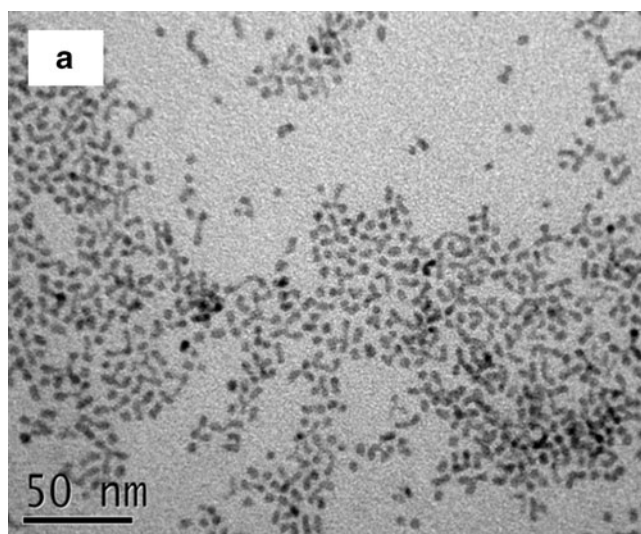
Fig. 2 **a** TEM micrograph of CdSe QDs sample, and **b** UV–vis absorption spectra

growth of particles during the displacement of capping groups by the polymer. Such red shifts are in reasonable agreement with results of other authors [14] for CdSe/PMMA nano fibers. Furthermore, it is clearly seen that there is an enhancement in the peak intensity as the concentration increase.

Figure (4) shows the UV–vis. and photoluminescence (PL) spectra of CdSe QDs. It is observed from this figure that the emission band edge at 590 nm shows a normal red shift of the emission from the absorption with small stokes shift (10 nm).

Figure (5) show the PL spectra of the same samples. From the figure, the increase in the concentration of the QDs had no significant effect on the peak positions, but only the intensity of the peaks increased with increasing the concentration. This indicated that there was no significant quantum dot growth at all concentrations after the casting process and thus this proves good quantum confinement properties of the QDs. Comparing the peak wavelength between CdSe QDs and PMMA(CdSe) film, there is also a red shift after the addition of CdSe QDs to PMMA. Moreover, the PL peak intensity is greatly enhanced, even increased nearly 2.5 times. Such an increase in PL peak intensity agrees reasonably with the results of other authors [4, 27]. In such study the increase in PL peak intensity could be attributed to possible chemical bonding between CdSe and carboxylate group of PMMA which cures the defect at the surface and hence better electron – hole recombination.

Thermal measurments

The PA signal amplitude was recorded at various f for each sample (depth profile analysis). The plots of ln PA amplitude versus the ln f are given in Fig. 6(a–d) for 0.001, 0.005, 0.01 and 0.05 wt.% concentrations respectively. The distinct change in the slope, at the characteristic frequency (f_c) where the crossover take place can be easily observed. Using Eq. (1), α was then calculated . Our thermal diffusivity value for the PMMA film without CdSe QDs addition was $1.12 \times 10^{-7} m^2/s$

Fig. 3 UV–vis. spectra of PMMA(CdSe) films with different QDs concentrations
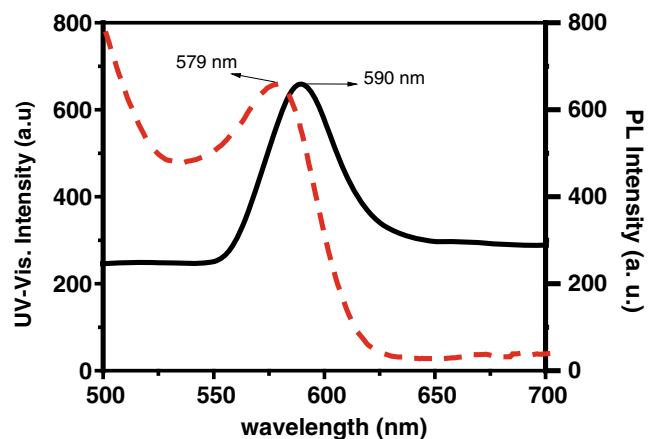

Fig. 4 UV–vis. absorption and PL of CdSe QDs
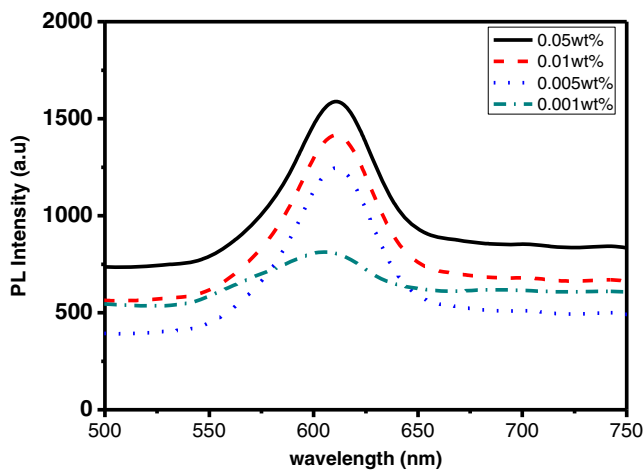
Fig. 5 PL spectra of the PMMA(CdSe) films with different QDs concentrations

which is very close to the reported value of α for PMMA ($\approx 1.11 \times 10^{-7} \, \mathrm{m^2/s}$) [28] . The variation of thermal diffusivity of PMMA(CdSe) composite films with CdSe concentrations is given in Fig. 7. The results showed that, there is an enhancement of α with increasing CdSe ratio which was 118 % from its

original value for the highest concentration. Figure 8 shows the experimental values of PA amplitude ratio ($R = q_s/q_r$) for the composite film, 0.001 wt.% CdSe QDs concentration, relative to the reference (Si wafer) as a function of $f^{1/2}$. The film and the reference were covered by an aluminum foil. Other samples show the same behavior. The satisfactory agreement between the experiment and calculations could be achieved by proper choice of fitting parameters e_s. The results showed that the values of e_s of PMMA(CdSe) increased from 666.4 $\mathrm{Ws^{1/2}/m^2}$ K to 955 $\mathrm{Ws^{1/2}/m^2K}$ as the concentration of CdSe QDs increase from 0.001 to 0.05 wt.%.

As mentioned before, the thermal parameters α and e are derived quantities depending on k and ρc in a different manner. The variations of ρc versus filler (QDs) content are weak. Consequently, the similar behavior of both quantities versus QDs loading clarify that the effect of QDs on these parameters is coming mainly from their effect on k. The measured values of α and e ($1.12 \times 10^{-7} \, \mathrm{m^2/s}$ and 633 $\mathrm{Ws^{1/2}\,m^{-2}K^{-1}}$) for the pure PMMA sample are used to calculate its thermal conductivity k ($e\sqrt{\alpha} = 0.22$) which is very close to the reported value of k for PMMA (0.21 W/mK) [29]. The measured values of k for our composite samples as a function of concentration of CdSe QDs are presented in Fig. 9. There is again an increase in k with
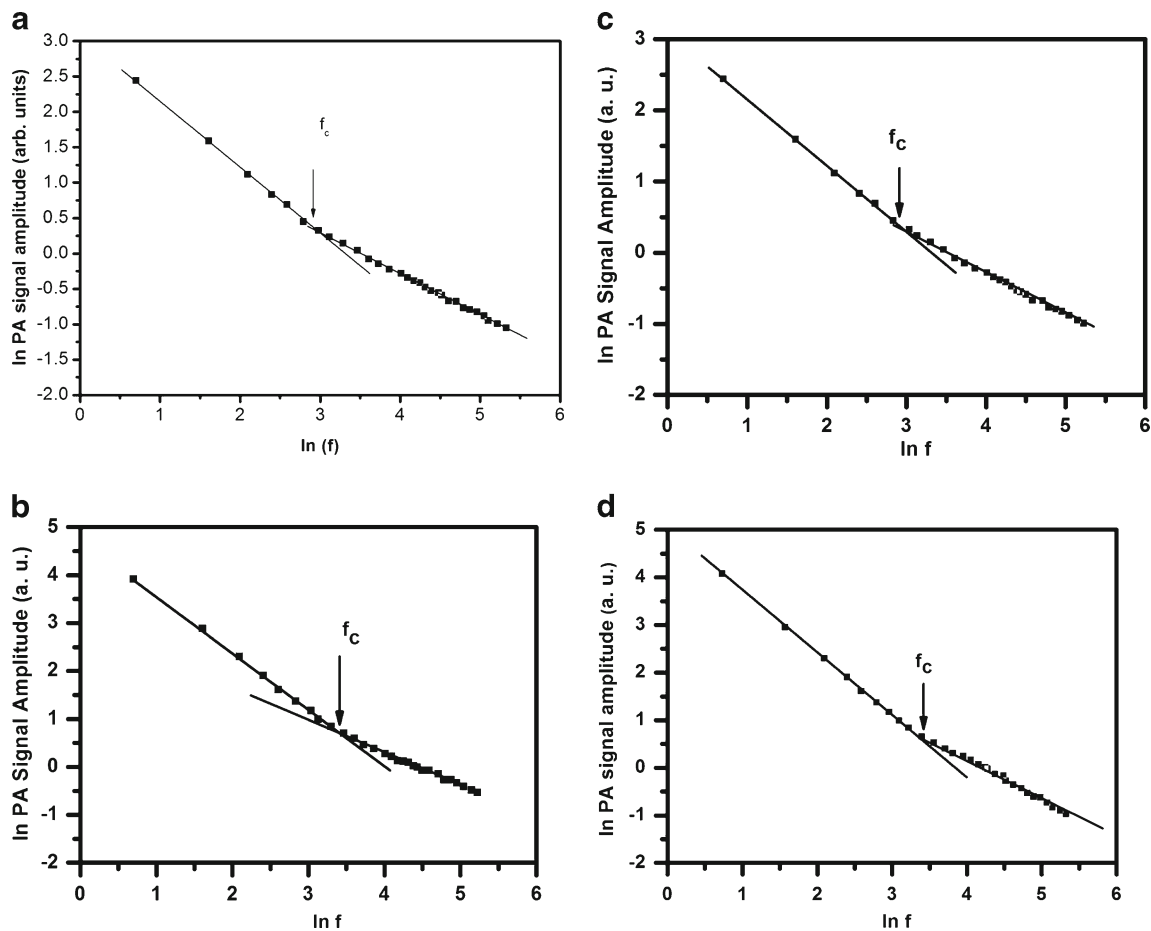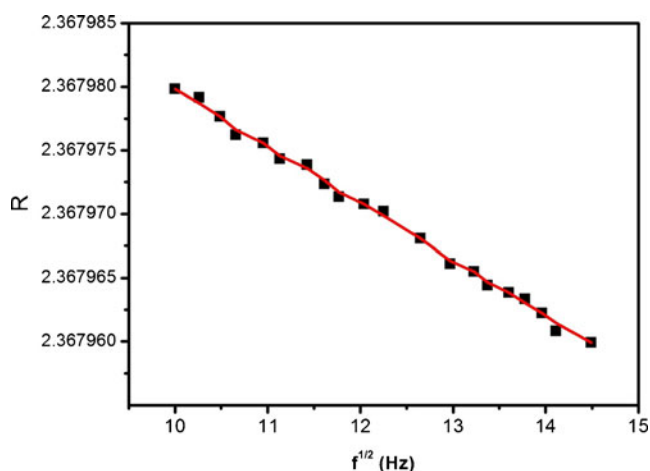

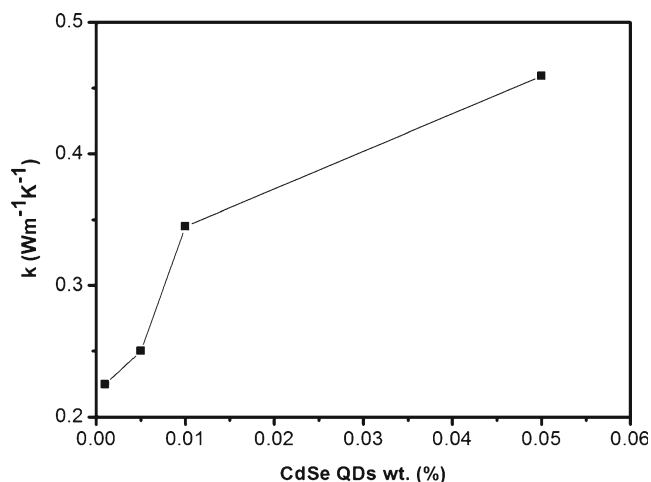**Fig. 6** ln PA amplitude vs. ln f for: **a** 0.001 wt.%, **b** 0.005 wt.%, **c** 0.01 wt.%, and **d** 0.05 wt.%
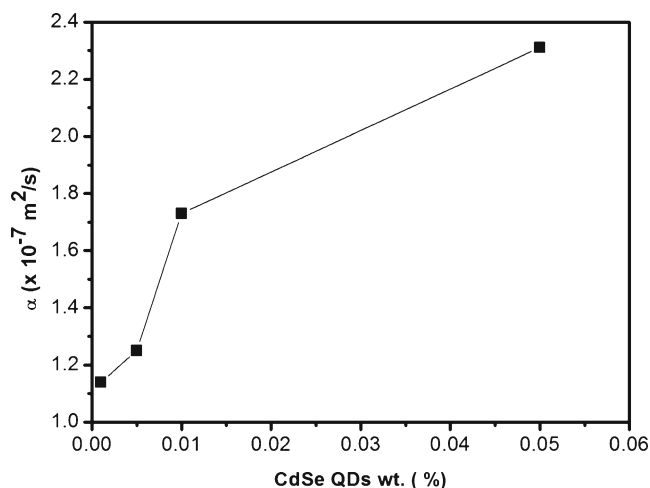
Fig. 7 Thermal diffusivity as a function of CdSe QDs weight percent

Fig. 9 Thermal conductivity as a function of CdSe QDs weight percentage

increasing QDs concentration. The increase in k is more significant (≈120 %) at the highest concentration 0.05 wt.% of QDs. Such an increase in k with increasing QDs concentration was reported by other authors [9]. In their work, they obtained an increase in k reach to ≈ 150 % for CNTs embedded in PVC. In our earlier work [30], the thermophysical properties of CdSe QDs were determined using PA technique. The results showed that the value of α, e and k were 4.21×10^{-5} m^2/s, 9,926 Ws$^{1/2}$m^{-2}K^{-1} and 64.41 W/mK, respectively. Therefore, the significant increases of composite thermophysical properties by adding a small amount of QDs were predicted. Incorporation of QDs into the PMMA matrix is accompanied by two opposite effects influencing heat transport in the composite. The first one is the appearance of a surface of a new phase increase the number of interfaces, which increase of phonon scattering reduce the heat flow transport, thus resulting in an interfacial resistance. The second effect is the presence of a volume of a new phase with high thermal conductivity, which results in an increase of the heat flow. Our results showed that, the second

effect became predominant at high QDs concentrations and these two effects are approximately equal for the low QDs concentrations.

Electrical conductivity

The temperature dependence of dc electrical conductivity for different concentrations (0.001 to 0.05 wt.%) is shown in Fig. 10. As can be seen, the electrical conductivity was slightly increased with increasing the concentration till certain temperature T_1. After this temperature, the conductivity was enhanced with increasing the temperature for all film composites and it became about four orders of magnitude for the highest QDs concentration (0.05 wt.%) compared with that of pure PMMA at 500 ^{0}C. This is an indication of an efficient incorporation of QDs inside the polymer matrix and a strong interaction between PMMA and QDs. This interaction increases significantly the electrical properties of the PMMA polymer after T_1. It is clear from Fig. 10, that the addition of

Fig. 8 PA amplitude ratio R versus $f^{1/2}$ for PMMA(CdSe) film of 0.001 wt.% concentration. The solid line is the best fit according to Eq. 2
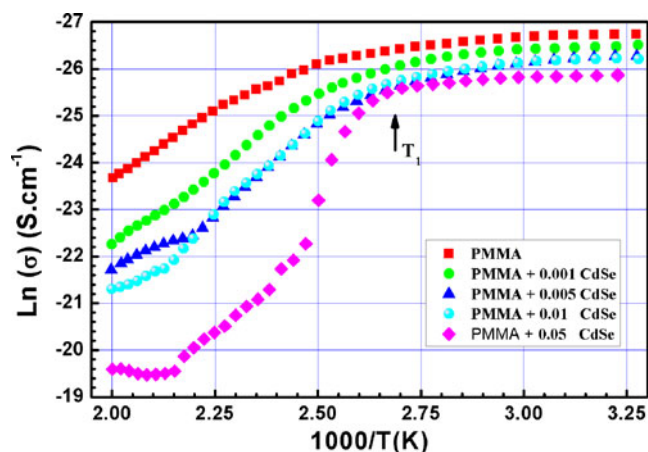

Fig. 10 The temperature dependence of dc electrical conductivity of pure and doped PMMA with different QDs concentrations

QDs into PMMA enhances the conductivity of the studied polymer under the effect of dc electric field.

Although the QDs ratio was very small it has a great effect on the dc electrical conductivity of the composite. As shown, the values of the electrical conductivity for the composites are higher than that of pure one. This refers to the facilitating of the conduction process through the presence of QDs, which either lie in the energy gap or act as donor and acceptor sites. These sites facilitate the hopping of electrons between valence and conduction bands and hence increasing the dc electrical conductivity[31]. The obtained conductivity values have also increased with increasing the temperature and this suggests that the electrical conductivity mechanism of the composites is a thermally activated hopping mechanism.

Conclusions

Composite films of PMMA(CdSe) has been fabricated with QDs loading 0.05 wt.% using casting technique. The observed red shifts of the absorption and PL edges of PMMA(CdSe) composite films from the CdSe QDs are due to the slight growth of particles. The increase in the concentration of the quantum dots had no significant effect on the peak positions, but only increased in the intensity of the peaks when the concentration was increased. Furthermore, the thermophysial parameters including α, e and k are obtained using PA technique. We demonstrate that a 120 % increase in k with QDs loading 0.05 %. Our results show that, the presence of new phases with high thermal conductivity is more dominant for high concentration. The electrical conductivity was enhanced about four orders of magnitude for the highest CdSe QDs concentration compared with pure PMMA. The obtained dc electrical conductivity values have increased with increasing the temperature and QDs concentration.

References

1. Patidar D, Rathore KS, Saxena NS, Sharma K, Sharma TP (2008) Energy band gap and conductivity measurments of CdSe Thin Films. Chalcogenide Lett 5:21–25

2. Dwivedi DK, Dayashankar, Dubey M (2009) Synthesis, Characeraization and Electrical Prperties of ZnTe Nanoparticles, Journal of Ovonic Research 5:35–41

3. Lan G-Y, Yang Z, Lin Y-W, Lin Z-H, Liao H-Y, Chang H-T (2009) A simple strategy for improving the energy conversion of multi-layered CdTe quantum dot-sensitized solar cells. J Mater Chem 19:2349–2355

4. Khanna PK, Singh N (2007) Light emitting CdS quantum dots in PMMA: synthesis and optical studies. J Lumin 127:474–482

5. Burroughes JH, Bradley DDC, Brown AR, Mark RN, Mackay K, Friend RH, Burns PL, Holmes AB (1990) Nature 347:539

6. Rubio-Ríos A, Aguilar-Castillo B, Flores-Gallardo S, Hernández-Escobar C, Zaragoza-Contreras E, Zhao Z, Carpenter M (2012) Effect of synthesis variables on the fluorescence properties of CdSe-polystyrene latexes. J Polym Res 19:1–7

7. Wang Z, Yang X, Wei J, Xu M, Tong L, Zhao R, Liu X (2012) Morphological, electrical, thermal and mechanical properties of phthalocyanine/multi-wall carbon nanotubes nanocomposites prepared by masterbatch dilution. J Polym Res 19:1–8

8. Lee J, Sundar VC, Heine JR, Bawendi MG, Jensen KF (2000) Full color emission from II–VI semiconductor quantum dot–polymer composites. Adv Mater 12:1102–1105

9. Aljaafari AA, Ibrahim SS, El-Brolossy TA (2011) Thermophysical and electrical characterization of PVC–SWNT nanocomposites. Compos Appl Sci Manuf 42:394–399

10. El-Brolossy T, Abdalla S, Hassanein OE, Negm S, Talaat H (2005) J Phys 125:685–688, IV Fr

11. George N (2002) Thermal diffusivity of liquid crystalline polymers measured using open cell photoacoustic technique. Smart Mater Struct 11:561–564

12. Selvan T, Spatz JP, Klok H, Möller M (1998) Gold-polypyrrole core-shell particles in diblock copolymer micelles. Adv Mater 10:132–134

13. Gaddy GA, Korchev AS, McLain JL, Slaten BL, Steigerwalt ES, Mills G (2004) J Phys Chem B 108:14850

14. Mthethwa TP, Moloto MJ, Vries AD, Matabola KP (2011) Properties of electrospum CdS and CdSe filled poly(methyl methacrylate) (PMMA) nanofibres. Mater Res Bull 46:569–575

15. Zhang Z, Shao C, Gao F, Li X, Liu Y (2010) Enhaced ultravuiolet emission from highly dispersed ZnO quantum dots embeded in poly(vinyl pyrrolidone) electrospum nanofibers. J Colloid Interface Sci 347:215–220

16. Rosencwaig A, Gersho A (1976) Theory of the photoacoustic effect with solids. J Appl Phys 47:65–69

17. Charpentier P, Lepoutre F, Bertrand L (1982) Photoacoustic measurements of thermal diffusivity description of the "drum effect". J Appl Phys 53:608–614

18. Abdelalim A, Abdallah S, Easawi K, Negm S, Talaat H (2010) Thermal properties of hydrated cement pastes studied by the photoacoustic technique. J Phys Conf Ser 214:012136

19. Raji P, Sanjeeviraja C, Ramachandran K (2004) Thermal properties of nano crystalline CdS. Cryst Res Technol 39:617–622

20. Sikorska A, Linde BBJ, Zwirbla W (2005) Study of thermal effusivity variations in water solutions of polyethylene glycol 200 using photoacoustic method. Chem Phys 320:31–36

21. Talapin DV, Haubold S, Rogach AL, Kornowski A, Haase M, Weller H (2001) A novel organometallic synthesis of highly luminescent cdte nanocrystals. J Phys Chem B 105:2260–2263

22. Davar F, Niasari MS, Baskoutasc S (2011) Appl Surf Sci 257:3872–3877

23. Badawi A, Al-Hosiny N, Abdallah S, Negm S, Talaat H (2012) Photoacoustic study of optical and thermal properties of CdTe quantum dots. J Mater Sci Eng A 2:1–6

24. Madelung O (2004) Semiconductors: data handbook, 3rd edn. Springer, Berlin

25. Kotkata MF, Masoud AE, Mohamed MB, Mahmoud EA (2009) Synthesis and structural characterization of CdS nanoparticles. Phys E: Low-Dimensional Syst Nanostruct 41:1457–1465

26. Pejova B, Tanuševski A, Grozdanov I (2004) Semiconducting thin films of zinc selenide quantum dots. J Solid State Chem 177:4785–4799

27. Cheng C, Wang S, Cheng X (2012) CdSe/PMMA: plastic fiber material containing CdSe quantum dots. Optics Laser Technol 44:1298–1300

28. Friederich B, AbdelghaniLaachachi M, Ferriol D, Ruch M, Cochez V (2010) Toniazzo, Tentative links between thermal diffusivity and fire-retardant properties in poly(methyl methacrylate) - metal oxide nanocomposites. Polym Degrad Stab 95:1183–1193

29. Han Z, Fina A (2011) Thermal conductivity of carbon nanotubes and their polymer nanocomposites: a review. Prog Polym Sci 36:914–944

30. Al-Hosiny N, Badawi A, Moussa MAA, El-Agmy R, Abdallah S (2012) Characterization of optical and thermal properties of CdSe quantum dots using photoacoustic technique. Int J Nanoparticles 5:258–266

31. Yakuphanoglua F, Yahia IS, Barim G, FilizSenkal B (2010) Double-walled carbon nanotube/polymer nanocomposites: electrical properties under dc and ac fields' Synth. Metals 160:1718–1726